ELSEVIER

Ceramics International 32 (2006) 207–211

CERAMICS INTERNATIONAL

www.elsevier.com/locate/ceramint

In situ synthesis and optical properties of strong red emitting nanomaterial: $Y_xGd_{2-x}O_3$: Eu^{3+} by composing different hybrid polymeric precursors

L. Zhou, B. Yan *

Department of Chemistry, Tongji University, Shanghai 200092, PR China

Received 3 July 2004; received in revised form 28 December 2004; accepted 2 February 2005
Available online 6 May 2005

Abstract

Nanometer-size $Y_xGd_{2-x}O_3$: Eu^{3+} with different ratio of Y and Gd (x = 0, 0.4, 1.0, 1.6, 2.0) were synthesized by using rare earth citric acid (CTA) or *iso*-nicotinic acid (PIC) coordination polymers as precursors for the luminescent species $Y_xGd_{2-x}O_3$: Eu^{3+}, composed with the polyethylene glycol (PEG) or poly methyl methacrylate (PMMA) both as dispersing media and fuel. Crystalline morphology and particle size were characterized by SEM and XRD, size distribution being in the range of 32–114 nm. Compared with the bulk Y_2O_3: Eu^{3+} phosphors, these nanometric materials show an especially strong emission of 611 nm and a blue shift of 7 nm. It is worthy pointing out that the emitting intensity of the phosphor reaches the strongest as the proportion of Y and Gd is 2–8.

Keywords: A. Powders: chemical preparation; C. Optical properties; D. Y_2O_3; E. Functional applications

1. Introduction

The essential requirements in display applications are the high-quality phosphors for sufficient brightness and long-term stability [1]. In order to improve the luminescent quantum efficiencies of phosphors, extensive research of effort has been devoted to the exceptional optical properties of rare-earth activated oxide phosphors because of their good luminescent characteristics, stability in high vacuum, and absence of corrosive gas emission under electron bombardment compared with currently used sulfide-based phosphors [2]. And thereby they were expected to act as potential kind of luminescent materials both for fundamental research and applications [3]. Yttrium doped with Eu ion is the most important and favorable phosphors due to its unsurpassed red emitting with high luminescence quantum efficiency in fluorescence lamps and projection television tubes [4–8]. Cubic Y_2O_3 for its chemical stability is an excellent host material for rare earth ions especially for Eu. Some reports indicate the relationship between the physical properties and the nano-size of Y_2O_3: Eu [9]. Yamaguchi et al. [10] found some weak satellite lines in the optical excitation spectra of $^7F_0 \rightarrow {}^5D_J$ in the Eu^{3+}: Y_2O_3 crystals. Yttrium and gadolinium oxide doped with Eu^{3+} are widely used as CRT and tricolor phosphors, a research has carried on the structure transition and its consequences on the luminescent properties of Eu^{3+} doped $Gd_{2-x}Y_xO_3$ nanocrystals fabricated by combustion method [11].

In this work, we report the preparation of the high red-emitting material: $Y_xGd_{2-x}O_3$: Eu^{3+}. The rare earth citrate (CTA) or *iso*-nicotinate (PIC) coordination polymers composed with organic polymer (polyethylene glycol (PEG) or poly methyl methacrylate (PMMA)) were used as the polymeric precursors. The thermal decomposition temperature is 600 °C. It is worthy to point that when the proportion of Y and Gd is 2–8, the emitting intensity of this phosphor rapidly increases. Comparing to the luminescent property of traditional bulk Y_2O_3: Eu^{3+} materials, these powders show strong emission at 611 nm.

---

* Corresponding author. Tel.: +86 21 65984663; fax: +86 21 65982287.
E-mail address: byan@tongji.edu.cn (B. Yan).

0272-8842/$30.00 © 2005 Elsevier Ltd and Techna Group S.r.l. All rights reserved.
doi:10.1016/j.ceramint.2005.02.010

2. Experimental

2.1. Synthesis of $Y_xGd_{2-x}O_3$: Eu^{3+}

The synthesis of $Y_xGd_{2-x}O_3$: Eu^{3+} by rare earth citrate coordination polymers—PEG precursors were described in the following way. Excess citric acid (5.0 mmol) over rare earth nitrates was dissolved into distilled water and its pH value was adjusted to be about 7.0 with ammonia solution. Then mixed solutions of rare earth nitrates ($Y(NO_3)_3$, $Gd(NO_3)_3$ and $Eu(NO_3)_3$) with different molar ratio were added and mixed homogenously. The aqueous solutions of urea ($0.3375\ \mathrm{mol\,l^{-1}}$, 10 ml) and PEG ($0.3375\ \mathrm{mol\,l^{-1}}$, 10 ml) were added into the above solutions and heated at 60 °C, whose pH value became alkalescence by dipping 1 mol% ammonia solution. After that, the temperature was increased to 100 °C to evaporate the excess solvent until the solution becomes viscous. It resulted in the hybrid precursors. It needs to be refereed that the thermolysis temperature was 600 °C to remove the organic component from rare earth coordination polymer systems. The typical scheme of the synthesis can be shown as below:

$$\begin{aligned}&x\mathrm{Y(NO_3)_3} + (2-x)\mathrm{Gd(NO_3)_3} + 0.02\mathrm{Eu(NO_3)_3}\\ &\quad + y\mathrm{CTA} + z\mathrm{NH_3\cdot H_2O} \rightarrow [\mathrm{RE(CTA)_3}]_n,\\ &\quad \text{coordination polymer} + m\mathrm{PEG} + n\mathrm{NH_2{-}CO{-}NH_2}\\ &\quad + z'\mathrm{NH_3\cdot H_2O} \rightarrow \mathrm{Y}_x\mathrm{Gd}_{2-x}\mathrm{O_3} : \mathrm{Eu^{3+}} + \mathrm{CO_2}\uparrow + \mathrm{H_2O}\uparrow\\ &\quad + \mathrm{NH_3}\uparrow + \mathrm{NO_2}\uparrow.\end{aligned}$$

The synthesis of $Y_xGd_{2-x}O_3$: Eu^{3+} by rare earth *iso*-nicotinic acid coordination polymers—PMMA precursors were adopted as the similar method except that the organic polymer was polymethyl methacrylate from the polymerization of its monomer (MMA) under the existence of the benzoyl peroxide (BPO) as initiator. The typical scheme of for the synthesis can be shown as below:

$$\begin{aligned}&x\mathrm{Y(NO_3)_3} + (2-x)\mathrm{Gd(NO_3)_3} + 0.02\mathrm{Eu(NO_3)_3}\\ &\quad + y\mathrm{HPIC} + z\mathrm{NH_3\cdot H_2O} + m'\mathrm{MMA(+BPO)}\\ &\quad \rightarrow [\mathrm{RE(PIC)_3}]_n\,\text{coordination polymer} + m\mathrm{PMMA}\\ &\quad + n\mathrm{NH_2{-}CO{-}NH_2} + z'\mathrm{NH_3\cdot H_2O} \rightarrow \mathrm{Y}_x\mathrm{Gd}_{2-x}\mathrm{O_3}:\mathrm{Eu^{3+}}\\ &\quad + \mathrm{CO_2}\uparrow + \mathrm{H_2O}\uparrow + \mathrm{NH_3}\uparrow + \mathrm{NO_2}\uparrow.\end{aligned}$$

2.2. Physical measurements of $Y_xGd_{2-x}O_3$: Eu^{3+}

The nanometer particles were characterized by means of X-ray powder diffraction (XRD, 40 kV and 20 mA, Cu Kα, Philips PW1710, reflections peaks for 2 2 0, 4 0 0, 4 4 0 and 6 2 0 directions were used in our measurements) and scanning electronic microscope (SEM, Philips XL-30). Excitation and emission spectra for solid powders of these phosphors were determined with Perkin-Elmer LS-55 model fluorophotometer (excitation wavelength 612 nm, scan rate 1000 nm/s, excitation slit width 10 nm, emission slit width 5 nm).

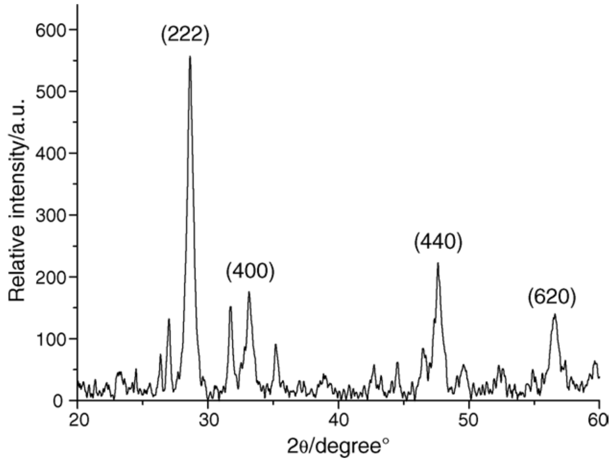

Fig. 1. XRD pattern of nanometer $Y_{0.4}Gd_{1.6}O_3$: Eu^{3+} by citrate coordination polymers—PEG precursors b (indexing of the above peaks according to ref. [15]).

3. Results and discussion

Fig. 1 shows the XRD pattern of nanometer $Y_{0.4}Gd_{1.6}O_3$: Eu^{3+} synthesized by rare earth citrate coordination polymers—PEG precursors (the representative indices peaks have been indicated and others belong to the same phase). The average crystallite size was estimated from the full width at half maximum of the diffraction peak by the Scherrer equation [12,13]:

$$D_{hkl} = k\lambda/[\beta(2\theta)\cos\theta] \tag{1}$$

where $\beta(2\theta)$ is the width of the pure diffraction profile in radians, k is the constant, 0.89, λ is the wavelength of the X-rays (0.154056 nm), θ is the diffraction angle, and D_{hkl} is the crystallite diameter in the $[h\,k\,l]$ direction. From the estimated data, it can be found that the nanometer $Y_xGd_{2-x}O_3$ materials have a size distribution in the range of 32–114 nm for rare earth citrate coordination polymers—PEG precursors and 26–135 nm for rare earth *iso*-nicotinic acid coordination polymers—PMMA precursors.

Due to the higher thermal decomposition temperature the crystallite size was larger than that reported in ref [14]. Of course, the larger size is also necessary and important to obtain the higher luminescence intensity. All the resultant products were well indexable as the Y_2O_3 cubic phase within the whole calication temperature range. For Gd_2O_3: Eu^{3+}, all the resultant products were also indexed to be Gd_2O_3 body-centered cubic phase similar to cubic Y_2O_3 for the lower thermal decomposition at 1200 °C [15]. The corresponding XRD pattern of nanometer $Y_{0.4}Gd_{1.6}O_3$: Eu^{3+} synthesized by rare earth *iso*-nicotinate coordination polymers—PMMA precursors show the similar feature to the above.

We further observed under the scanning electron microscope (SEM) selected nanometer $Y_xGd_{2-x}O_3$: Eu^{3+} samples (as shown in Fig. 2 for the $Y_{0.4}Gd_{1.6}O_3$: Eu^{3+} samples from rare earth *iso*-nicotinate-PMMA). There exist some conglomeration phenomena in SEM diagram for the

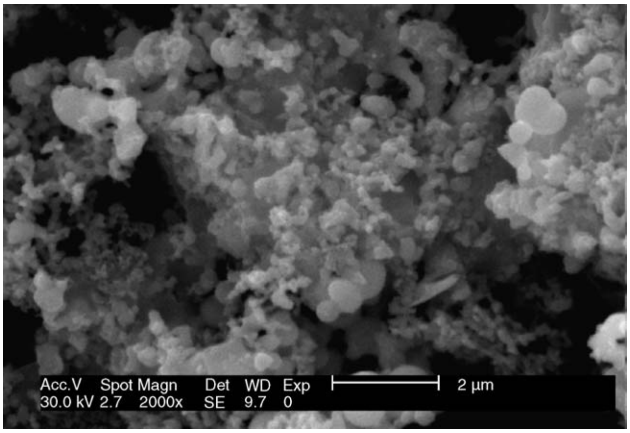

Fig. 2. SEM of nanometer $YGdO_3$: Eu^{3+} synthesized by *iso*-nicotinate coordination polymers—PMMA precursors.

higher thermolysis temperature. The uniformity of the nanophosphors morphology is not very good. From the SEM, it can be found that there are smaller granules in the sheet phosphors and can be predicted unintelligible the crystalline particle is in the size smaller than 100 nm, which agrees with the data from the XRD estimation. The phosphors by rare earth citrate show similar feature except for a higher agglomeration size.

Rare earth coordination polymers with citric acid and *iso*-nicotinic acid show the polymeric structure [16] and are used as the precursors to prepare the luminescent species. The organic polymers, PEG and PMMA were combined both as dispersing medium and fuel to form the polymeric hybrid precursor template with nanometer size and show higher temperature of thermolysis process. Rare earth citrates form three-dimensional polymeric network structure and rare earth *iso*-nicotinates belong to one-dimensional polymeric chain-like structure [16,17]. These coordination polymers can compose with organic polymers (PEG or PMMA) to obtain an interpenetrating polymeric network structures for they show the similar infinite polymeric structure. Therefore, the particle sizes of rare earth oxides (Y_2O_3, Gd_2O_3 and Eu_2O_3) can be controlled and determined by the structures of hybrid precursors. From the XRD and SEM, we can also find that the two different hybrid polymeric precursors have not too markedly influence on the micro morphology characteristics of calcinations products for they form the similar hybrid polymeric network. We suppose that this preparation technology connects the assembly of hybrid material with and synthesis of nanometer material, and can be expected to be a candidate to apply into the synthesis of other luminescent materials based with rare earth oxides.

The excitations spectra (200–280 nm) of the red luminescence ($\lambda_{em} = 612$ nm) show asymmetric band for all these $Y_xGd_{2-x}O_3$: Eu^{3+} nanophosphors. Figs. 3 and 5 show the excitation spectra of $Y_xGd_{2-x}O_3$: Eu^{3+} ($x = 0.4, 1, 1.6$) synthesized by citrate coordination polymers—PEG precursors and nanometer $Y_xGd_{2-x}O_3$: Eu^{3+} ($x = 0.4, 1, 1.6$) synthesized by *iso*-nicotinate coordination polymer—PMMA precursors, respectively. For the typical species $Y_{0.4}Gd_{1.6}O_3$: Eu^{3+} derived from citrate three excitation peaks were observed obviously at 224, 245 and 254 nm, respectively and for $Y_{0.4}Gd_{1.6}O_3$: Eu^{3+} derived from *iso*-nicotinate coordination polymers—PMMA precursors, two peaks appear at 245 and 253 nm, respectively, and the other peaks are too weak to be observed separately. All of these excitation bands are attributed to the transition towards the charge transfer state due to Eu–O interaction ($4f^72p^{-1}$ charge transfer band CTB) lying in the band gap region of the host matrix.

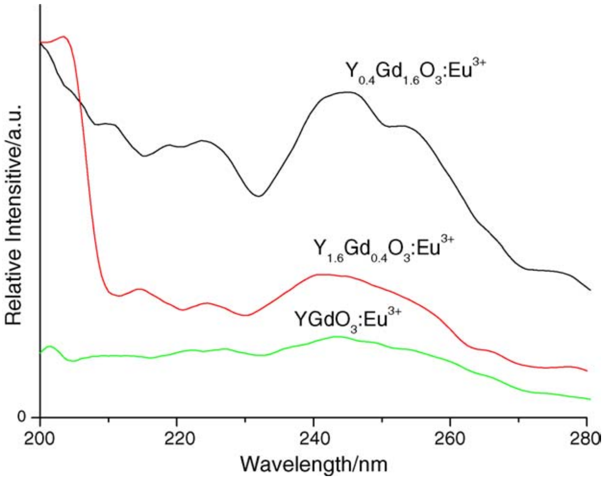

Fig. 3. Excitation spectra of nanometer $Y_xGd_{2-x}O_3$: Eu^{3+} by citrate coordination polymers—PEG precursors.

Figs. 4 and 6 show the corresponding emission spectra of nanometer $Y_xGd_{2-x}O_3$: Eu^{3+} with different molar ratio of Y to Gd by the two kinds of hybrid precursors. Both of which exhibit the characteristic luminescence originated from the transitions between the excited $^5D_0$ level and ^7F_J ($J = 0, 1, 2, 3, 4$) level of the $^4F_6$ configuration of the Eu^{3+} ion. The strongest emission peaks all are located at 611 nm,

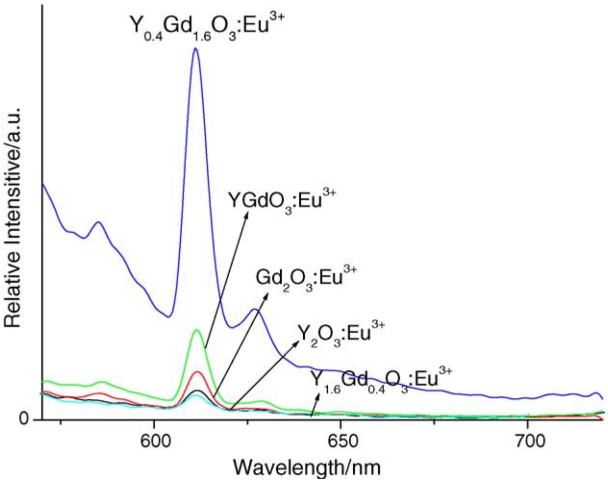

Fig. 4. Emission spectra of nanometer $Y_xGd_{2-x}O_3$: Eu^{3+} by citrate coordination polymers—PEG precursors.

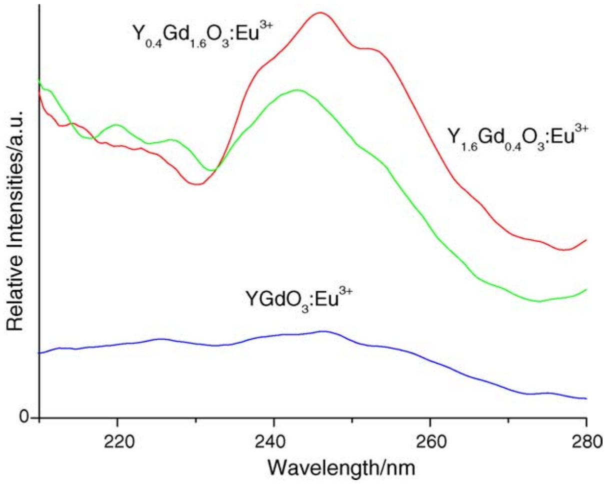

Fig. 5. Excitation spectra of nanometer $Y_xGd_{2-x}O_3$: Eu^{3+} synthesized by *iso*-nicotinate coordination polymers—PMMA precursors.

corresponding to the typical hypersensitive transition $^5D_0 \rightarrow {}^7F_2$ for Eu^{3+} ion, which is parity forbidden f–f intraconfigurational transition. In the body-centered cubic type Y_2O_3 and Gd_2O_3, there are two types of cationic sites occupied by RE^{3+} having either C2 or S6 local symmetries [14]. The former site lacking inversion center is quite favorable for observing the electric dipole transition as a forced transition due to the admixture of the odd parity states, whereas the latter is unfavorable for the electric dipole transition due to the presence of the inversion center. The minor emission component in the orange region around 580 nm due to the $^5D_0 \rightarrow {}^7F_1$ magnetic dipole transition is structurally independent. For this reason, this transition can be used as an internal stand to gain some idea of the relative transition strengths of the other transitions of Eu^{3+} [14]. Because of the limited resolution of the apparatus in our limited measurements, it was not possible for us to observe clearly in order to obtain enough information on the possible multiple sites occupied by Eu^{3+}.

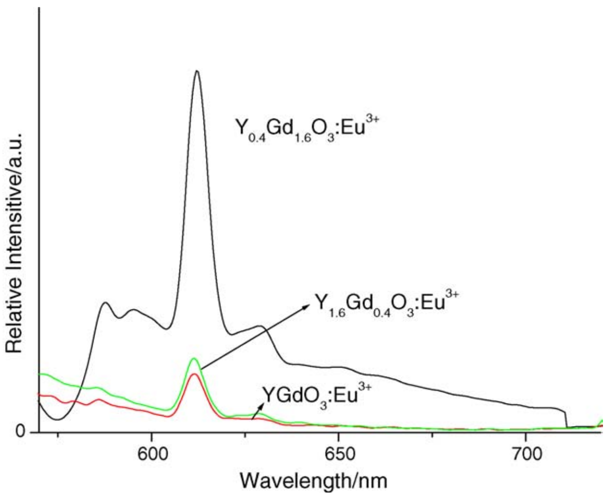

Fig. 6. Emission spectra of nanometer $Y_xGd_{2-x}O_3$: Eu^{3+} synthesized by *iso*-nicotinate coordination polymers—PMMA precursors.

Compare of relative intensities for different molar ratio of Y to Gd, it is found that the luminescence reaches the strongest intensity when the molar ratio of Y to Gd is 0.4–1.6, and its luminescence intensity was much stronger than that of other molar ratio of Y to Gd.

4. Conclusions

In summary, the synthesis of $Y_xGd_{2-x}O_3$: Eu^{3+} nanophosphors was achieved under 600 °C by assembling two kinds of hybrid polymeric precursors. The particle size is in the range of 30–40 nm. The photoluminescent properties show both of them exhibit the characteristic emission of Eu^{3+} ion and band shift to 611 nm. Comparing the luminescence intensities of $Y_xGd_{2-x}O_3$: Eu^{3+} with different molar ratio of Y to Gd, $Y_{0.4}Gd_{1.6}O_3$: Eu^{3+} belongs to the optimum ratio and possesses the strongest luminescence. Which indicates it is a candidate technology for the synthesis of nanometer rare earth oxides.

Acknowledgement

The authors are supported by the Science Foundation of Shanghai Universities for Excellent Youth Scientists.

References

[1] M.G. Kwak, J.H. Park, S.H. Shon, Synthesis and properties of luminescent Y_2O_3: Eu (15–25 wt%) nanocrystals, Solid State Commun. 130 (2004) 199.

[2] R.C. Ropp, The Chemistry of Artificial Lighting Devices: Lamps, Phosphors, and Cathode Ray Tubes, Elsevier, New York, 1993.

[3] L.D. Sun, C.S. Liao, C.H. Yan, Structure transition and enhanced photoluminescence of $Gd_{2-x}Y_xO_3$: Eu nanocrystals, J. Solid State Chem. 171 (2003) 304.

[4] G. Tessari, M. Bettinelli, A. Speghini, D. Ajo, G. Pozza, L.E. Depero, B. Allieri, L. Sangaletti, Synthesis and optical properties of nanosized powders: lanthanide-doped Y_2O_3, Appl. Surf. Sci. 144–145 (1999) 686.

[5] W.Y. Jia, Y.Y. Wang, F. Fernandez, X.J. Wang, S.H. Huang, W.M. Yen, Photoluminescence of Ce^{3+}, Tb^{3+}: Y_2O_3 nanoclusters embedded in SiO_2 sol–gel glasses, Mater. Sci. Eng. C 16 (2001) 55.

[6] R. Schmechel, M. Kennedy, H.V. Seggern, H. Winkler, M. Kolbe, R.A. Fischer, X.M. Li, A. Benker, M. Winterer, H. Hahn, Luminescence properties of nanocrystalline Y_2O_3: Eu^{3+} in different host materials, J. Appl. Phys. 89 (2001) 1679.

[7] G. Wakefield, E. Holland, P.J. Dobson, Luminescence properties of nanocrystalline Y_2O_3: Eu, Adv. Mater. 13 (2001) 1557.

[8] A.P. Bartko, L.A. Peyser, R.M. Dickson, A. Mehta, T. Thundat, R. Bhargava, M.D. Barnes, Observation of dipolar emission patterns from isolated Eu^{3+}: Y_2O_3 doped nanocrystals: new evidence for single ion luminescence, Chem. Phys. Lett. 358 (2002) 459.

[9] Q. Li, L. Gao, D.S. Yan, Effects of grain size on wavelength of Y_2O_3: Eu^{3+} emission spectra, NanoStruct. Mater. 8 (1997) 825.

[10] M. Yamaguchi, K. Koyama, T. Suemoto, Three-parameter mapping of site distribution by optical-RF double resonance in Eu_{3+}: Y_2O_3 crystals, J. Lumin. 87–89 (2000) 1099.

[11] G.S. Wu, Y. Lin, X.Y. Yuan, T. Xie, B.C. Cheng, L.D. Zhang, Novel synthesis route to Y_2O_3: Eu nanotubes, Nanotechnology 15 (2004) 568.

[12] H.P. Klug, L.E. Alexander, X-ray Diffraction Procedures for Polycrystalline and Amorphous Materials, John Wiley & Sons Inc., New York, 1974.

[13] R. Jenkins, R.L. Snyder, Introduction to X-ray Powder Diffractometry, John Wiley & Sons Inc., New York, 1996.

[14] J. Dhanaraj, R. Jagannathan, T.R.N. Kutty, C.H. Lu, Photoluminescence characteristics of Y_2O_3: Eu^{3+} nanophosphors prepared using sol–gel thermolysis, J. Phys. Chem. B. 105 (2001) 11098.

[15] T. Ye, G.W. Zhao, W.P. Zhang, S.D. Xia, Combustion synthesis and photoluminescence of nanocrystalline Y_2O_3: Eu phosphors, Mater. Res. Bull. 32 (1997) 501.

[16] C.B. Yuan, D.Q. Zhao, Y.J. Wu, F.K. Pei, J.Z. Liu, J.Z. Ni, C-13 NMR study on the aqueous structure of lanthanide citrate complexes, Acta Chim. Sin. 56 (1996) 581.

[17] B. Yan, Q.Y. Xie, A novel unexpected seven-coordinated chain-like dysprosium coordination polymer of pyridine-4-carboxylate: structure and photophysical property, Inorg. Chem. Commun. 6 (2003) 1448.